

NO_x reduction on a transition metal-free γ -Al₂O₃ catalyst using dimethylether (DME)

Emrah Ozensoy^a, Darrel Herling^b, János Szanyi^{b,*}

^a *Bilkent University, Department of Chemistry and Institute of Material Science and Nanotechnology, 06800 Ankara, Turkey*

^b *Institute for Interfacial Catalysis, Pacific Northwest National Laboratory, P.O. Box 999, MSIN K8-80, Richland, WA 99352, United States*

Available online 31 January 2008

Abstract

NO₂ and dimethylether (DME) adsorption as well as DME and NO₂ co-adsorption on a transition metal-free γ -alumina catalyst were investigated via in-situ transmission Fourier transform infrared spectroscopy (in-situ FTIR), residual gas analysis (RGA) and temperature programmed desorption (TPD) techniques. NO₂ adsorption at room temperature leads to the formation of surface nitrates and nitrites. DME adsorption on the alumina surface at 300 K leads to molecularly adsorbed DME, molecularly adsorbed methanol and surface methoxides. Upon heating the DME-exposed alumina to 500–600 K the surface is dominated by methoxide groups. At higher temperatures methoxide groups are converted into formates. At $T > 510$ K, formate decomposition takes place to form H₂O(g) and CO(g). DME and NO₂ co-adsorption at 423 K does not indicate a significant reaction between DME and NO₂. However, in similar experiments at 573 K, fast reaction occurs and the methoxides present at 573 K before the NO₂ adsorption are converted into formates, simultaneously with the formation of isocyanates. Under these conditions, NCO can further be hydrolyzed into isocyanic acid or ammonia with the help of water which is generated during the formate formation, decomposition and/or NCO formation steps.

© 2008 Elsevier B.V. All rights reserved.

Keywords: NO_x reduction; SCR; Al₂O₃; NO₂; Nitrate; Nitrite; Formate; Methoxy; FTIR; TPD; Dimethylether (DME); Methanol; Solid acid catalyst

1. Introduction

Dimethylether (CH₃OCH₃, DME) is a widely utilized commodity chemical which is also projected to be one of the fundamental chemical feedstocks in the future [1]. DME is non-toxic, non-carcinogenic, non-teratogenic (i.e. not causing developmental malformations) and non-mutagenic [2,3]. Thus, it is currently commonly used in aerosol propellants, diesel additives and refrigerants in the industry. DME has also a potential to substitute liquefied petroleum gas (LPG) for household applications as a clean fuel [4]. In addition, DME can also be used in diesel-engine vehicles with minor fuel system modifications as DME use results in thermal efficiencies comparable to traditional fuel, lower NO_x emission, near zero smoke production and less engine noise [5,6]. Furthermore, DME can also be exploited in hydrogen powered energy applications as an efficient hydrogen carrier. This can be

achieved using a hybrid catalyst in a two-step process. First, DME is hydrolyzed over a solid acid catalyst to methanol (MeOH) and then hydrogen is produced from methanol through steam reforming (SR) over Cu/ZnO/ γ -Al₂O₃ [7,8].

Mass production of DME can be achieved through coal or natural gas [1] or using methanol dehydration over solid acid catalysts such as alumina or H-ZSM-5 [7,9–11]. As it can be inferred from the discussion above, DME → MeOH and MeOH → DME reactions can be both catalyzed in a reversible fashion on solid acid catalysts. Therefore, DME and methanol reactions on solid acid catalysts have a large number of similarities [9–40].

Recently, application of DME as a reducing agent in selective catalytic reduction of NO_x in diesel-powered engines has also been suggested [38]. Therefore, in the current work, we have investigated the interaction of DME and NO₂ on a γ -Al₂O₃ catalyst in a temperature interval that is relevant to NO_x reduction applications (300–630 K) via in-situ transmission Fourier transform infrared spectroscopy (in-situ FTIR), residual gas analysis (RGA) and temperature programmed desorption (TPD) techniques. Surface species, gas phase

* Corresponding author. Tel.: +1 509 371 6524; fax: +1 509 376 5106.

E-mail address: janos.szanyi@pnl.gov (J. Szanyi).

products and various aspects of the surface reaction mechanisms relevant to the transformations of these species on one of the most commonly used catalyst support materials, i.e. Al_2O_3 [1–48], are discussed.

2. Experimental

The infrared measurements were carried out in transmission mode, using a Nicolet Magna 750 spectrometer equipped with an MCT detector operating at 4 cm^{-1} resolution. Prior to each spectral series acquisition, a background spectrum was taken of the clean, adsorbate-free sample. The in-situ infrared cell used in the experiments was a $2^{3/4}$ in six-way stainless steel cube equipped with KBr IR-windows. The cell is connected to a gas handling/pumping station and through both leak and gate valves to a quadrupole mass spectrometer (UTI 100C). The base pressure of the cell was less than 1×10^{-6} Torr, and the maximum pressure attainable was 1000 Torr. The catalyst sample was pressed onto a fine tungsten mesh, which, in turn, was mounted onto a copper sample holder assembly attached to ceramic feedthroughs of a 1.33 inch flange. This set up allowed heating of the samples to 1000 K and cooling to cryogenic temperatures. The sample temperature was monitored through a chromel/alumel (K-type) thermocouple spot-welded to the top center of the tungsten mesh. After the sample was mounted in the IR cell, it was gradually heated to 773 K in vacuum and kept at that temperature for about 2 h to ensure the removal of water from the catalyst. (We also commonly baked the IR cell and the gas manifold during dehydration to minimize the readsorption of water from the walls of the IR cell onto the catalyst surface upon completion of the annealing). In a typical experiment, the sample held at a given temperature was exposed to various gases and the changes in the IR spectra were followed as a function of time or temperature. The in-situ FTIR experiments were conducted in batch (constant pressure) mode. $\text{NO}_2(\text{g})$ and $\text{DME}(\text{g})$ used in the experiments were typically purified further via multiple freeze-thaw-pump steps before the experiments. In the TPD experiments, a typical linear heating rate of 12 K/min was used.

3. Results and discussion

3.1. NO_2 adsorption on $\gamma\text{-Al}_2\text{O}_3$

Fig. 1 illustrates the IR results of the NO_2 adsorption experiments on the γ -alumina catalyst. For the series of experiments shown in Fig. 1, $\text{NO}_2(\text{g})$ (9.7 Torr) was introduced onto the fresh catalyst at room temperature. After the establishment of a steady gas pressure reading, the reactor was evacuated. Next, IR spectra were obtained during temperature programmed heating of the catalyst from 310 to 620 K in vacuum. Spectra were taken at sample temperature increments of 20 K (with the exception of the 340 K spectrum which was collected after the 330 K one). Fig. 1a presents a detailed view of the complex nature of the IR features of the adsorbed NO_x species. The spectral window within 1200–1650 cm^{-1} yields a large number of overlapping IR features.

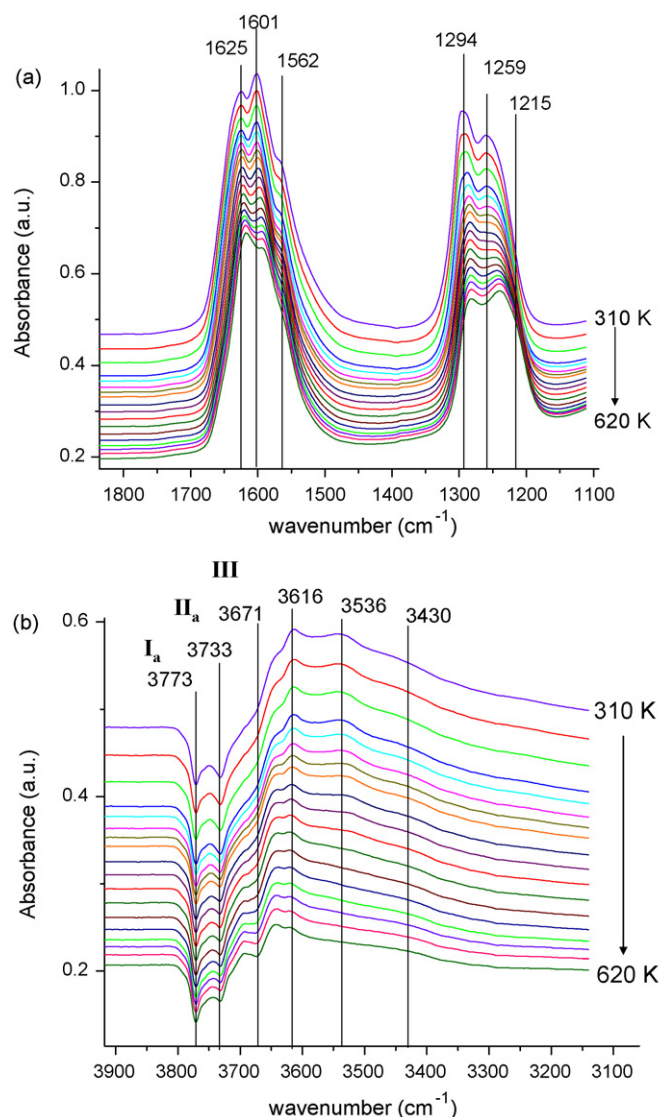
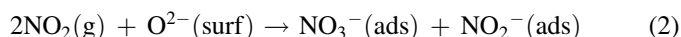
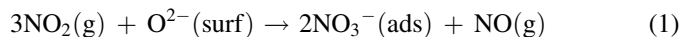
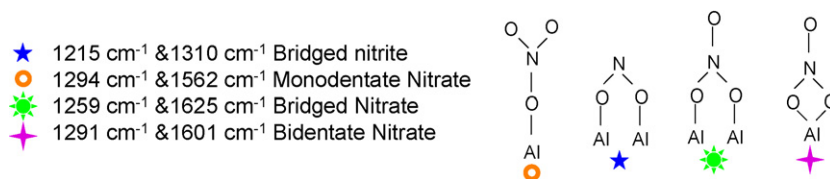


Fig. 1. In-situ FTIR spectra for NO_2 adsorption on γ -alumina. For the series of spectra given here, 9.7 Torr of NO_2 was dosed on the catalyst surface at room temperature followed by evacuation at room temperature. Next, FTIR spectra were acquired at the given temperatures in vacuum: (a) 1700–1100 cm^{-1} region and (b) 3800–3200 cm^{-1} region.

Some of the distinguishable features are observed at 1215, 1259, 1294, 1562, 1601 and 1625 cm^{-1} . Such a behavior is well known in the literature [28,30,47] for NO_x adsorption on alumina surfaces where complex and convoluted bands are observed due to the formation of surface nitrites and nitrates through the following routes [30,47]:



Based on the results of previous reports [28,30,41,47], we assign the 1215 cm^{-1} feature to bridged nitrite, 1294 and 1562 cm^{-1} features to monodentate nitrate, 1259 and 1625 cm^{-1} features to bridged nitrate and finally 1291 and 1601 cm^{-1} features to bidentate nitrate species (Scheme 1).



Scheme 1. Types of NO_x species formed during NO_2 adsorption on Al_2O_3 .

Fig. 1b shows the spectral window within $3200\text{--}3800\text{ cm}^{-1}$ for the same series as it is displayed in Fig. 1a. It is clear that the formation of nitrates and nitrites upon NO_2 adsorption on the γ -alumina surface is accompanied by the appearance of a broad positive feature within $3400\text{--}3600\text{ cm}^{-1}$ which is concomitant with negative features developing between 3670 and 3790 cm^{-1} . Although it is difficult to obtain quantitative information regarding the relative abundances of these transformed hydroxyl species, our results are consistent with former studies where similar negative features were commonly observed during the adsorption of various probe molecules on alumina. It was reported that the vibrational frequencies of these features are virtually invariant for different probe molecules [12,14–17,22–24,37,42–44]. In these extensive former reports, the formation of these negative IR bands were attributed to the interaction of isolated hydroxyl groups on the alumina surface with the probe molecule, which resulted in the disappearance of the isolated OH groups and the appearance of a broad IR band within $3400\text{--}3600\text{ cm}^{-1}$, implying the formation of hydrogen bonded surface hydroxyl groups. These former studies [12,14–17,22–24,37,42–44] can guide us to assign the types of isolated surface hydroxyl groups which are interacting with the surface NO_x species that are formed upon NO_2 adsorption. Considering the frequency values of these negative features, it can be argued that NO_x species interact with the different types of OH groups (I_a, II_a, and III) discussed in detail by Knozinger and Ratnasamy [43]. The series of spectra in Fig. 1b also indicates that with increasing temperature, the intensity of the broad hydrogen bonded O–H vibrational features decreases significantly, while that of the negative features remains practically unchanged. This suggests, that the originally present (prior to NO_2 introduction) surface hydroxyl groups interact with NO_x in two different ways: (1) NO_x adsorption on these hydroxyls that results in the redshift of the ν_{OH} bands (development of the broad IR feature between 3200 and 3400 cm^{-1}), and (2) reaction between ionic NO_x species and the surface hydroxyls that actually results in the removal of H^+ and/or OH^- from the alumina surface. Both processes bring about the disappearance of the original ν_{OH} vibrations. However, upon heating the NO_2 -saturated alumina sample, and as the hydrogen bonded hydroxyls lose their intensities, the corresponding surface hydroxyl vibrational features should recover their intensities. What we see here, in contrast, is that the original hydroxyl vibrations do not recover in any noticeable extent, suggesting that the most of the original surface hydroxyls actually reacted with the NO_2 , and after the TPD experiment the number of surface hydroxyls are significantly reduced in comparison to the initial ones. This has been proposed in our previous combined FTIR/TPD study of NO_2 interaction with $\gamma\text{-Al}_2\text{O}_3$ sample where we observed the desorption of H_2O as the

NO_x species evolved in the TPD process [47]. The simultaneous occurrence of these two processes (i.e. H-bonding and chemical reaction) makes it very difficult to correlate the NO_x features (nitrites and nitrates) with the negative features of surface hydroxyls.

Desorption of the adsorbed NO_x on this alumina surface was also monitored with TPD. In short, TPD experiments suggested two major NO_x desorption channels at 370 and 760 K , where the desorbed species were in the form of $\text{NO} + \text{NO}_2$ for the low temperature channel (N_2O_3 desorption and decomposition), whereas, for the high temperature channel NO_2 desorption (almost exclusively) from the decomposition of surface nitrates were observed. In addition, water desorption was also observed simultaneously with the high temperature NO_x desorption. The results of these experiments are in complete agreement with our previous detailed study on NO_2 adsorption on $\gamma\text{-Al}_2\text{O}_3$ surface [47].

3.2. DME adsorption on $\gamma\text{-Al}_2\text{O}_3$

DME adsorption on this γ -alumina catalyst was studied with in-situ IR spectroscopy. Fig. 2a presents the results for 3.4 Torr of DME adsorption on the fresh catalyst at room temperature, followed by evacuation of the reactor at the same temperature and then acquisition of IR spectra at the given temperatures, in vacuum. During the temperature ramp, an IR spectrum was recorded at every 20 K temperature increment within 300 and 630 K (with the exception of the first temperature increment which was 30 K). Fig. 2a displays IR spectra in the $1000\text{--}4000\text{ cm}^{-1}$ region that were collected as a function of sample temperature (from 300 to 630 K) after room temperature DME exposure of the γ -alumina catalyst. Panels b–d of Fig. 2 present detailed views of selected spectra from the same experiment for different spectral ranges. Fig. 2a clearly indicates that the temperature dependent DME adsorption spectra can be divided into three different spectral sections: $1100\text{--}1800\text{ cm}^{-1}$ (b), $2700\text{--}3100\text{ cm}^{-1}$ (c) and $3200\text{--}3800\text{ cm}^{-1}$ (d).

The top spectrum in Fig. 2b was collected at 300 K and comprises a number of strong features. Based on the previous detailed reports on methanol [12,25,46], formaldehyde [29,46] and dimethylether [40] adsorption on alumina surfaces, we assign the features at c.a. 1473 , 1460 and 1430 cm^{-1} to $\delta_{\text{as}}(\text{CH}_3)$ of Type I' bridging methoxide [25,46], $\delta_{\text{s}}(\text{CH}_3)$ of Type I' bridging methoxide [25,46] and $\delta_{\text{s}}(\text{OH})$ of Type II or Type III adsorbed methanol groups [25,46], respectively. It should be noted that, as a result of the minor differences in the vibrational frequencies in the C–H stretching region ($2700\text{--}3100\text{ cm}^{-1}$), it is difficult to differentiate the C–H stretching modes of methoxide and molecularly adsorbed methanol

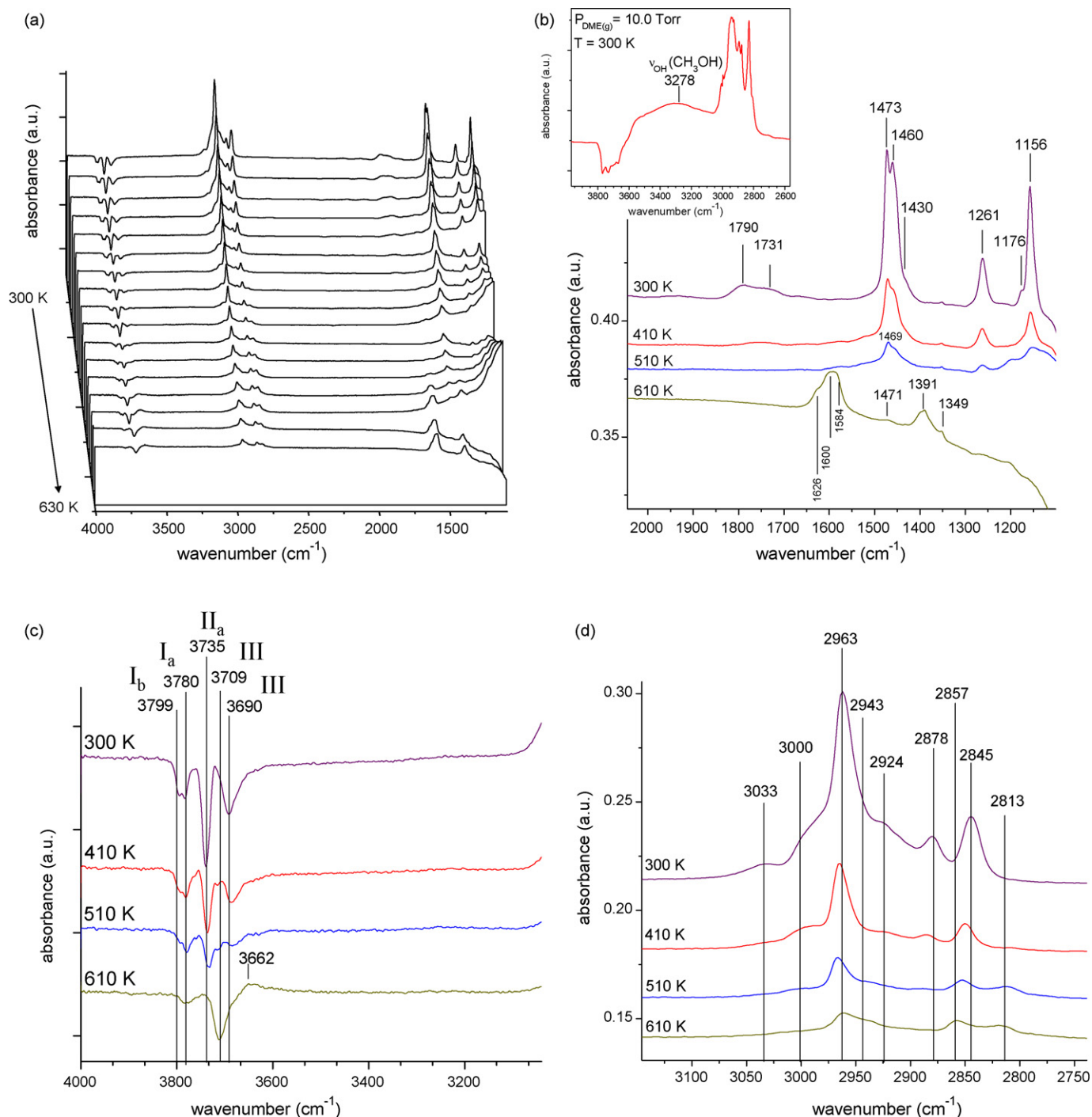


Fig. 2. In-situ FTIR spectra for DME adsorption on γ -alumina. For the series of spectra given here, 3.4 Torr of DME was dosed onto the catalyst at room temperature followed by evacuation at room temperature. Next, FTIR spectra were acquired at the given temperatures in vacuum. (a) 1000–4000 cm^{-1} , (b) 2000–1100 cm^{-1} region, (c) 4000–3100 cm^{-1} region and (d) 3100–2750 cm^{-1} region. The inset of b presents a separate experiment emphasizing the existence of a broad and low frequency $\nu(\text{OH})$ stretching feature at $\sim 3278 \text{ cm}^{-1}$ (due to molecularly adsorbed methanol species), during the DME adsorption at 300 K, where 10.0 Torr DME was dosed on a fresh catalyst and IR spectra were acquired without evacuation.

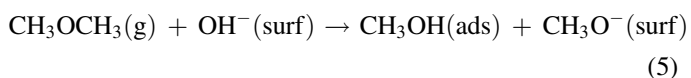
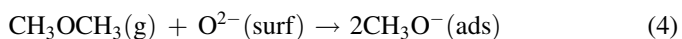
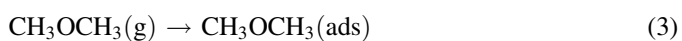
species (Fig. 2d). On the other hand, the presence of a broad and a low frequency $\nu(\text{O-H})$ mode around 3278 cm^{-1} (see also inset of Fig. 2b) strongly indicates the presence of adsorbed methanol on the surface [18]. The feature at 1156 cm^{-1} can be attributed to molecularly adsorbed DME [40] or a coordinated methanol species [46]. Based on the results of a former inelastic neutron scattering spectroscopy (INS) study [40], we tenta-

tively assign the 1176, 1261, 1790 and 1731 cm^{-1} features to weakly bound molecularly adsorbed DME species. These features, in addition to the other features associated with molecularly adsorbed species loose their intensities significantly at 410 K and almost completely disappear at 510 K, in accordance with previous observations on DME adsorption on alumina surfaces [40]. At 510 K, as Fig. 2b clearly indicates,

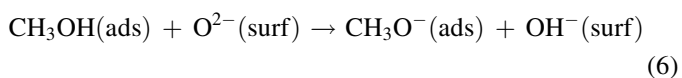
the surface is dominated by methoxide species. Increasing the temperature to 610 K leads to a profound change in the IR spectrum and yields new features within c.a. 1630–1570 and c.a. 1400–1330 cm^{-1} . The bands at 1600 and 1584 cm^{-1} can readily be assigned to $\nu_{\text{as}}(\text{CO}_2^-)$ modes of formate species [29]. In a similar manner, bands at 1391 and 1349 cm^{-1} can be assigned to $\delta(\text{CH})$ of the same species [29]. Furthermore, a shoulder located at 1626 cm^{-1} can be observed which can be attributed to hydroxyl bending modes of adsorbed H_2O (see below for details).

Fig. 2c focuses on the changes in the O–H stretching region of the vibrational spectra (3000–3800 cm^{-1}) during the course of DME adsorption on the alumina catalyst. It is apparent from Fig. 2c that within 300–510 K, surface species formed as a result of DME adsorption interact with four different isolated hydroxyl groups of Types I_a, I_b, II_a and III, [43] on the catalyst. Contrary to NO_2 adsorption (Fig. 1b), disappearance of these isolated hydroxyls are not accompanied with the formation of hydrogen bonded –OH groups around 3500 cm^{-1} , suggesting that DME adsorption results in a proton transfer from the isolated hydroxyls to other surface species, i.e. O–H bond scission. Within 300–510 K, the increasing temperature leads to the attenuation of these negative peaks, pointing to the partial regeneration of these isolated hydroxyls via thermal decomposition of various surface species. At 610 K, concomitant with the formation of surface formates (Fig. 2b), a noticeable decrease in the Type III isolated hydroxyls are evident.

Fig. 2a–d provides very important complimentary information which can be utilized to further elaborate on the DME adsorption on the γ -alumina catalyst. It is apparent that DME adsorption on the alumina catalyst at 300 K leads to three major adsorption products, which are molecularly adsorbed DME, molecularly adsorbed methanol and methoxides, possibly via the following pathways:



Consumption of surface hydroxyl groups in pathway (5) is consistent with the appearance of negative hydroxyl bands in Fig. 2a and c, suggesting hydroxyl-assisted dissociative DME adsorption yielding adsorbed methanol and methoxides. At 410–510 K most of the molecularly adsorbed DME and methanol decomposes via pathways (3)–(5) and also through:



Pathway (6) is also in line with the disappearance of negative hydroxyl features (i.e. partial regeneration of surface hydroxyl groups) within 410–510 K as a result of hydroxide production. At temperatures higher than 510 K, the methoxy

groups can be converted into formates, in accordance with the mechanism that was discussed in Ref. [18] over $\eta\text{-Al}_2\text{O}_3$. As it was also substantiated by the results of our gas phase analysis with both IR and RGA (data not shown here), formate production is accompanied by gas phase methane and probably hydrogen formation. Then at higher temperatures the produced formates can further decompose to yield H_2O and CO.

3.3. DME + NO_2 sequential co-adsorption on $\gamma\text{-Al}_2\text{O}_3$ catalyst at 423 K

After having investigated the adsorption of NO_2 and DME on the γ -alumina catalyst separately, their co-adsorption was also examined at two sample temperatures (423 and 573 K), where DME adsorption yielded methoxide species with some molecularly adsorbed methanol as we have discussed above. For the series of spectra presented in Fig. 3, first 5.0 Torr of DME(g) was introduced onto a fresh catalyst at 423 K and then the evolution of the IR spectra was monitored for 60 s, showing that DME quickly reaches equilibrium on the surface. At $t = 61$ s, 10.0 Torr of NO_2 was added to the reactor and FTIR spectra were recorded continuously for 10 min. It is evident from Fig. 3 that, in accordance with the results discussed above, DME adsorption at 423 K yields features corresponding to methoxide, methanol and gas phase DME in addition to a small amount of DME(ads). Upon the introduction of $\text{NO}_2(\text{g})$, immediate increases in the intensities of the nitrite/nitrate features and a simultaneous attenuation of the carbon-containing surface species are observed. This is readily visible by the reduction in the intensities of the C–H stretching features within 2750–3050 cm^{-1} in Fig. 3. In addition, the IR band of $\text{NO}_2(\text{g})$ at c.a. 1610 cm^{-1} is also distinguishable, although, it overlaps with the nitrate peaks. These changes in the IR spectra point to the fact that at 423 K the primary surface process is substitution of adsorbed DME/ CH_3OH fragments by NO_x species. Minor reactions, however, cannot be excluded to take place on the surface, and they are evidenced by the development of small bands at 2256 and 1925 cm^{-1} . The feature at 2256 cm^{-1} can be attributed to isocyanate ($-\text{NCO}$) species which are formed on the surface (see Section 4 for details). Although the intensity of the $-\text{NCO}$ feature slightly increases with time, it is still quite minor with respect to the other surface species seen in Fig. 3. Another minor feature observed at 1925 cm^{-1} can be associated with NO coordinated on the metal (Al^{3+}) cations of the alumina surface which is a product of NO_2 dissociation on the surface or NO adsorption as a result of gas phase decomposition of NO_2 [46]. Alternatively, the same feature can be associated with the presence of adsorbed N_2O_3 , originating from the reaction between $\text{NO}_2(\text{g})$ and $\text{NO}(\text{g})$ that is the decomposition product of NO_2 [47]. Therefore, in general, in-situ IR spectra given in Fig. 3 suggest that at 423 K, strongly adsorbed NO_x species form on the alumina surface. These NO_x species (mostly nitrates) displace a large fraction of the adsorbed organic fragments, while reaction between NO_x and the DME fragments is very limited.

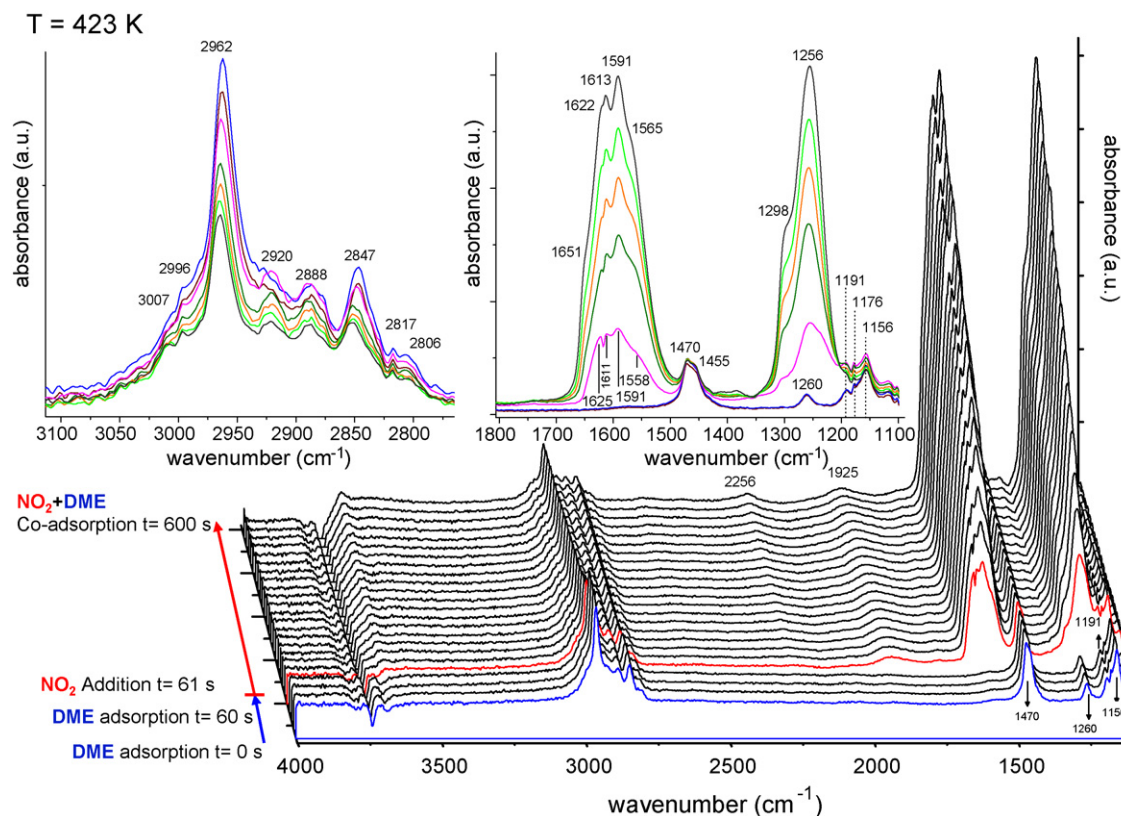


Fig. 3. Time-dependent in-situ FTIR data for the sequential DME and NO_2 co-adsorption on γ -alumina at 423 K. For this series of experiments, 5.0 Torr of DME(g) was introduced onto a fresh catalyst at 423 K. Next, at $t = 61$ s, 10.0 Torr of NO_2 was added to the reactor at 423 K. Spectra were obtained without evacuation.

3.4. DME + NO_2 sequential co-adsorption on $\gamma\text{-Al}_2\text{O}_3$ at 573 K

DME and NO_2 co-adsorption experiments were also performed on γ -alumina at 573 K. In these series of experiments, as in the co-adsorption experiments performed at 423 K, 5.0 Torr of DME was first introduced on a fresh catalyst at 573 K. Next, IR spectra were collected under these conditions for the first 60 s. At $t = 61$ s, 10.0 Torr of NO_2 was dosed to the system and IR spectra were collected for 10 min. The results of this experiment are summarized in Fig. 4a for the entire spectral range recorded ($1000\text{--}4000\text{ cm}^{-1}$). Spectra in the $1000\text{--}2600\text{ cm}^{-1}$ region collected at different stages of this experiment are shown in Fig. 4b. The bottommost spectrum in Fig. 4b corresponds to the surface of the catalyst immediately after the introduction of DME at 573 K. The most prominent feature of the spectrum is the band at 1465 cm^{-1} which is associated with the surface methoxides. Contrary to the series of spectra given in the inset of Fig. 2b, the lack of a broad feature at around 3200 cm^{-1} suggests the lack of molecularly adsorbed methanol under these conditions. Since molecularly adsorbed DME is not stable at high temperatures (although gas phase DME is visible in the IR spectra by considering the band centered at 1176 cm^{-1}), surface is dominated by methoxide species at $t = 0$ s. As time elapses, at $t = 60$ s, formation of two weak bands at 1597 and 1325 cm^{-1} can be seen which are attributed to the generation of formates [29]. At $t = 61$ s, with the introduction of $\text{NO}_2(\text{g})$ to the reactor, profound changes in

the IR spectra are observed. The methoxide feature at 1465 cm^{-1} slightly decreased whereas the formation of three very strong bands is noticed. These features are centered at 1391 , 1596 and 2254 cm^{-1} and can be assigned to $\nu_{\text{as}}(\text{CO}_2^-)$ and $\delta(\text{CH})$ modes of formate species [29] and to isocyanates ($-\text{NCO}$), respectively [46]. Besides these features, IR bands associated with gas phase species are also visible in Fig. 4b which are due to $\text{NO}(\text{g})$ (1876 cm^{-1}), $\text{NO}_2(\text{g})$ (shoulder at 1610 cm^{-1}), DME(g) (1176 cm^{-1}), CO (2143 cm^{-1}), CO_2 (2347 cm^{-1}) and may be even $\text{HNCO}(\text{g})$ (2251 cm^{-1}) convoluted with the $\text{NCO}(\text{ads})$ band.

Although nitrates are the major surface species observed in the IR spectra in the sequential co-adsorption of DME and NO_2 on the alumina surface at 423 K, at 573 K the IR spectra reveal the presence of no such species on the surface. This might also be due to the rapid conversion of nitrites/nitrates into other surface or gas phase species at 573 K, which may occur in a time scale that is significantly faster than the time scale of the IR data acquisition.

Fig. 4c focuses on the C–H and O–H stretching regions of the series of spectra given in Fig. 4b. It is apparent from Fig. 4c that there are changes in the C–H stretching region upon the introduction of NO_2 on the catalyst surface at 573 K. Specifically, intensities of the peaks at 2894 , 2929 and 3006 cm^{-1} increase while those of the peaks at 2961 and 2849 cm^{-1} decrease. The bands at 2961 and 2849 cm^{-1} can be assigned to the $\nu(\text{CH}_3)$ stretching modes of methoxides [25] whereas, the bands at 2929 and 3006 cm^{-1} can be associated

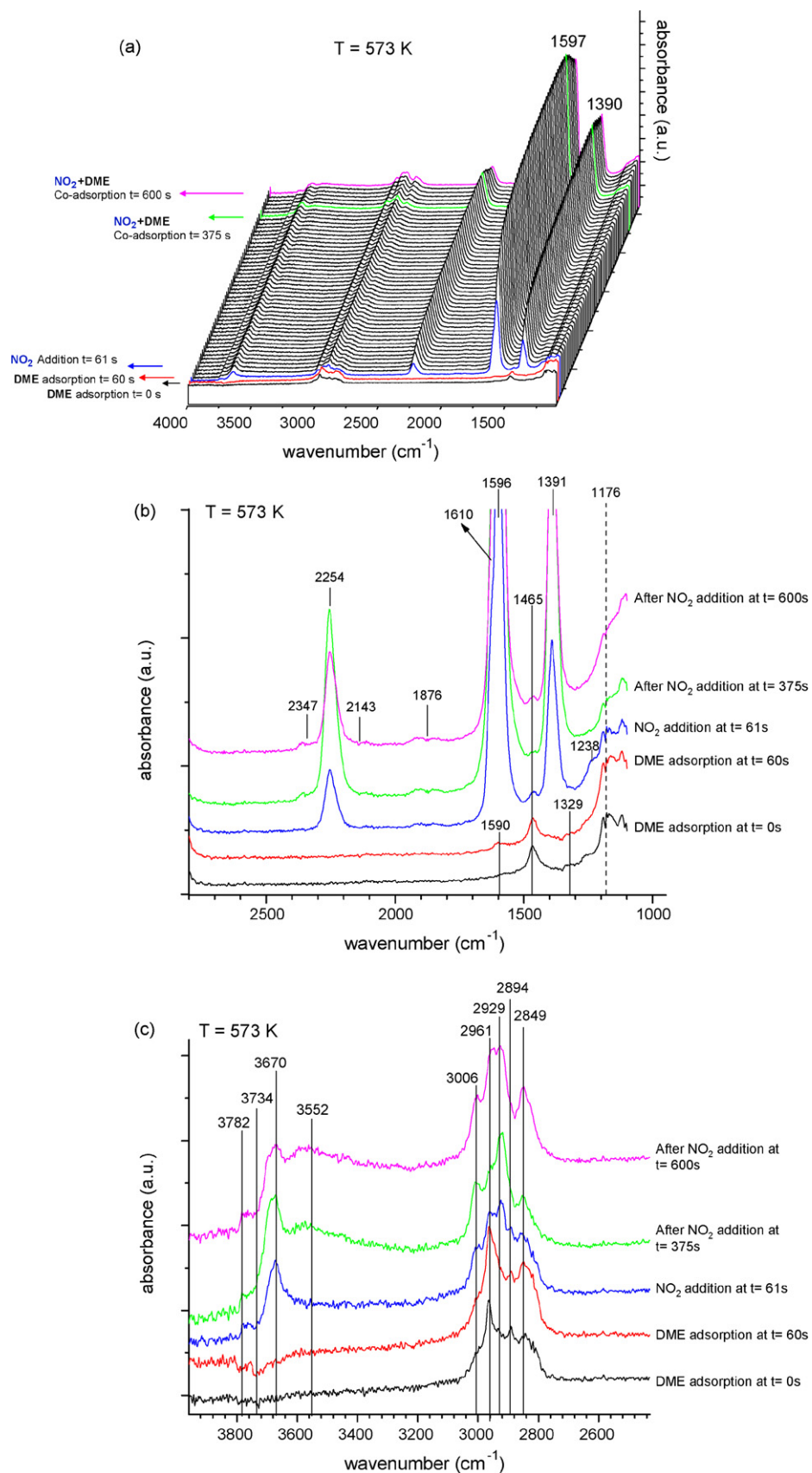
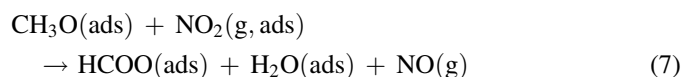


Fig. 4. Time-dependent in-situ FTIR data for the sequential DME and NO_2 co-adsorption on γ -alumina at 573 K. For this series of experiments, 5.0 Torr of DME(g) was introduced onto a fresh catalyst at 573 K. Next, at $t = 61 \text{ s}$, 10.0 Torr of NO_2 was added to the reactor at 573 K. Spectra were obtained without evacuation. (a) 1000–400 cm^{-1} region, (b) 2700–1000 cm^{-1} region and (c) 3800–2600 cm^{-1} region.

with formates (the minor band at 2894 cm^{-1} may also be attributed to gas phase methanol or DME). These changes in the C–H spectral region are accompanied by transformations in the O–H stretching region. Increases in the intensities of Type III (3670 cm^{-1}) and Type I_a (3782 cm^{-1}) isolated hydroxyls as well as the accentuation of hydrogen bonded hydroxyl groups at 3552 cm^{-1} towards the later stages of co-adsorption and reaction of DME and NO_2 on the catalyst surface.

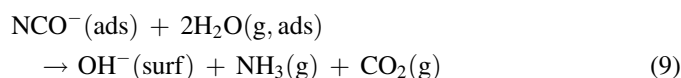
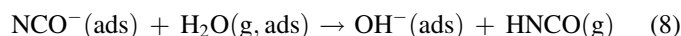
Another important aspect of the series of spectra given in Fig. 4a is that the growth of the NCO and the formate features and the concomitant attenuation of the methoxide features are not monotonic in time and a reversal of these intensity trends are observed after a certain period. At the later stages of the DME + NO_2 experiment, a decrease in the formate bands and the simultaneous recovery of the methoxide bands are observed (Fig. 4c).

In the light of the information that is provided by Fig. 4a–c, the chemical transformations that are occurring during the sequential adsorption of DME and NO_2 at 573 K can be rationalized. The conversion of surface methoxides (that are formed upon DME adsorption at 573 K on the alumina surface) to formates occur after the addition of NO_2 through the following pathway where gas phase (or adsorbed NO_2) reacts with methoxides to form formates, adsorbed water and NO:



This pathway is also consistent with the increase in the hydroxyl features given in Fig. 4a and b upon addition of $\text{NO}_2(\text{g})$ to the reactor. Furthermore, an increase in the $\text{NO}(\text{g})$ feature at 1876 cm^{-1} in Fig. 4b during the latter stages of NO_2 addition is also in accord with the suggested pathway. The formation of surface isocyanates (NCO) (the development of the broad IR band centered at 2255 cm^{-1}) closely follows the formation of adsorbed formates. How these NCO species form is not clear at this point. They might be produced in the reaction of the formates with some type of NO_x species, or they may form directly in the reaction of methoxides with NO_x . Note that as the gas phase NO_2 is consumed, the intensities of the characteristic IR bands of both the formate and NCO species begin to drop. Concomitantly, increases in the intensities of IR bands of the methoxy groups (2961 and 2848 cm^{-1}) are seen after the consumption of all the gas phase NO_2 , since there is still unreacted DME present in the IR cell.

It is well known in the literature that adsorbed isocyanate species are quite reactive in the presence of water and quickly hydrolyze into isocyanic acid or in the presence of excess water into ammonia on the alumina surface via [48,49]:



Isocyanic acid in gas phase results in an IR band centered at 2255 cm^{-1} . Therefore a contribution from isocyanic acid in addition to surface isocyanate groups cannot be ruled out

considering the asymmetric feature located at 2254 cm^{-1} in Fig. 4b. The small quantities of $\text{NH}_3(\text{g})$ produced in pathway (9) can readily react with NO_x species present in order to form NH_4NO_2 and NH_4NO_3 species that can play important roles in the reduction of NO_x . The hydrolysis of the NCO groups can yield isocyanic acid and/or ammonia and carbon dioxide. (Clear evidence for the hydrolysis reaction to produce CO_2 and NH_3 can be seen in panel b of Fig. 4 as the intensity of the characteristic gas phase CO_2 feature at 2347 increases with time-on-stream. The vibrations of the produced ammonia in the gas phase (1630 and 3334 cm^{-1}) cannot be distinguished since they overlap with the other strong vibrations in the spectra (Fig. 4b–c).)

Therefore, by analyzing the results presented in Fig. 4a–c, it can be suggested that at 573 K, DME adsorption on the fresh γ -alumina catalyst leads to mostly methoxides with a small amount of formates on the surface. Addition of $\text{NO}_2(\text{g})$ to the reactor causes transformation of surface methoxides to formates and causes NCO production. Meanwhile, produced formates can also decompose to form carbon monoxide and water. Considering the rapid attenuation of the NCO peak in line with the consumption of NO_x species in the reactor, it is likely that isocyanates are highly reactive at 573 K. Hydrolysis of isocyanates under these conditions suggests formation of isocyanic acid and ammonia. Ammonia formation during the NO_2 + DME interaction is very important as it provides a NO_x reduction path to the catalytic system. It is also important to note that unlike with many transition metal-containing catalytic systems, such as three-way catalysts (Pt, Rh and Pd supported with γ -alumina) where isocyanate formation during NO_x reduction ($\text{NO} + \text{CO}$ reaction) is typically suggested to occur first on the metal sites followed by a spill-over on the oxide support [49–51], in the current work, we present evidence for significant amount of isocyanate formation directly on the oxide surface (i.e. γ -alumina) in the absence of a metal binding site.

4. Summary and conclusion

In this work we investigated NO_2 , DME adsorption and sequential DME and NO_2 co-adsorption on γ -alumina catalyst that is relevant to NO_x reduction applications (300–630 K). Our experimental results can be summarized as follows:

- NO_2 adsorption on the γ -alumina catalyst leads to the formation of surface nitrates and nitrites, in agreement with the results of previous studies on similar systems. Produced nitrates and nitrites desorb from the surface via multiple pathways, mostly in the form of $\text{NO} + \text{NO}_2$ at low temperature, and as NO_2 at high temperature. The high temperature nitrate decomposition is also accompanied by water desorption resulting in the partial dehydroxylation of the alumina surface.
- DME adsorption on the alumina surface at 300 K leads to molecularly adsorbed DME, molecularly adsorbed methanol and methoxides. Within 500–600 K the surface is dominated by methoxide groups. However, at higher

temperatures methoxide groups are converted into formates opening up further reaction paths for decomposition. At $T > 600$ K, formate decomposition was observed in the form of $\text{H}_2\text{O}(\text{g})$ and $\text{CO}(\text{g})$.

- (c) Sequential DME and NO_2 co-adsorption at 423 K mostly results in competitive adsorption on the surface where an adsorbate substitutes the other one, however IR results do not indicate a significant reaction between DME and NO_2 at 423 K. On the other hand, similar experiments at 573 K suggest a fast reaction where the methoxides present at 573 K before the NO_2 adsorption are converted into formates simultaneously with the formation of isocyanate. Under these conditions, NCO can further be hydrolyzed into isocyanic acid or ammonia with the help of water which is generated during the formate formation and decomposition steps.

Acknowledgements

We gratefully acknowledge the US Department of Energy (DOE), Office of Basic Energy Sciences, Division of Chemical Sciences for the support of this work. The research described in this paper was performed in the Environmental Molecular Sciences Laboratory (EMSL), a national scientific user facility sponsored by the DOE Office of Biological and Environmental Research and located at Pacific Northwest National Laboratory (PNNL). PNNL is operated for the US DOE by Battelle Memorial Institute under contract number DE-AC05-76RL01830. E.O. acknowledges the support from the Scientific and Technical Research Council of Turkey (TUBITAK) (Project Code: 105Y260).

References

- [1] Y. Fu, T. Hong, J. Chen, A. Auroux, J. Shen, *Thermochim. Acta* 434 (2005) 22.
- [2] T.A. Semelsberger, K.C. Ott, R.L. Borup, H.L. Greene, *Appl. Catal. B* 61 (2005) 281.
- [3] Dupont, Dymel Aerosol Propellants, Product Information, 1995.
- [4] M. Sun, L. Yu, C. Sun, Y. Song, J. Sun, *Gen. Rev.* 20 (2003) 695.
- [5] M. Xu, J.H. Lunsford, D.W. Goodman, A. Bhattacharyya, *Appl. Catal. A* 149 (1997) 289.
- [6] A.M. Rouhi, *Chem. Eng. News* May 29 (1995).
- [7] T. Takeguchi, K.-I. Yanagisawa, T. Inui, M. Inoue, *Appl. Catal. A* 192 (2000) 201.
- [8] J. Topp-Jorgensen, US Patent 4,536,485 (1985).
- [9] J.-H. Kim, M.J. Park, S.J. Kim, O.-S. Joo, K.-D. Jung, *Appl. Catal. A* 264 (2004) 37.
- [10] G. Pagani, US Patent 4,098,809 (1978).
- [11] G.C. Chinchin, J.R. Jennings, US Patent 4,863,894 (1989).
- [12] G. Busca, *Catal. Today* 27 (1996) 457.
- [13] G. Busca, *Catal. Today* 32 (1996) 133.
- [14] G. Busca, *Catal. Today* 41 (1998) 191.
- [15] G. Busca, *Phys. Chem. Chem. Phys.* 1 (1999) 723.
- [16] K. Sohlberg, S.T. Pantelides, S.J. Pennycook, *J. Am. Chem. Soc.* 123 (2001) 26.
- [17] D.T. Lundie, A.R. McInroy, R. Marshall, J.M. Winfield, P. Jones, C.C. Dudman, S.F. Parker, C. Mitchell, D. Lennon, *J. Phys. Chem. B* 109 (2005) 11592.
- [18] A.R. McInroy, D.T. Lundie, J.M. Winfield, C.C. Dudman, P. Jones, D. Lennon, *Langmuir* 21 (2005) 11092.
- [19] M. Trombetta, G. Busca, S. Rossini, V. Piccoli, U. Cornaro, A. Guercio, R. Catani, R.J. Willey, *J. Catal.* 179 (1998) 581.
- [20] D.T. Wickham, B.W. Logsdon, S.W. Cowley, C.D. Butler, *J. Catal.* 128 (1991) 198.
- [21] E.E. Miro, G. Imoberdorf, J. Vassallo, J.O. Petunchi, *Appl. Catal. B* 22 (1999) 305.
- [22] X. Liu, R.E. Truitt, *J. Am. Chem. Soc.* 119 (1997) 9856.
- [23] D. Dautzenberg, H. Knozinger, *J. Catal.* 33 (1974) 142.
- [24] H. Knozinger, K. Kochloeff, W. Meye, *J. Catal.* 28 (1973) 69.
- [25] G. Busca, P.F. Rossi, V. Lorenzelli, M. Benaissa, J. Travert, J.C. Lavalley, *J. Phys. Chem.* 89 (1985) 5433.
- [26] E.C. Decanio, V.P. Nero, J.W. Bruno, *J. Catal.* 135 (1992) 444.
- [27] S. Schaueremann, J. Hoffmann, V. Johaneck, J. Hartmann, J. Libuda, *Phys. Chem. Chem. Phys.* 4 (2002) 3909.
- [28] B. Westerberg, E. Fridell, *J. Mol. Catal. A* 165 (2001) 249.
- [29] G. Busca, J. Lamotte, J.C. Lavalley, V. Lorenzelli, *J. Am. Chem. Soc.* 109 (1987) 5197.
- [30] C. Paze, G. Gubitosa, S.O. Giacone, G. Spoto, F.X.L. Xamena, A. Zecchina, *Top. Catal.* 30–31 (2004) 169.
- [31] Q. Wu, H. He, Y. Yu, *Appl. Catal. B* 61 (2005) 107.
- [32] P.A. Clayborne, T.C. Nelson, T.C. Devore, *Appl. Catal. A* 257 (2004) 225.
- [33] V.V. Galvita, G.L. Semin, V.D. Belyaev, T.M. Yurieva, V.A. Sobyanyin, *Appl. Catal. A* 216 (2001) 85.
- [34] K.W. Jun, H.S. Lee, H.S. Roh, S.E. Park, *Bull. Korean Chem. Soc.* 23 (2002) 803.
- [35] S.Y. Nishimura, R.F. Gibbons, N.J. Tro, *J. Phys. Chem. B* 102 (1998) 6831.
- [36] R.S. Schiffino, R.P. Merrill, *J. Phys. Chem.* 97 (1993) 6425.
- [37] C. Morterra, G. Magnacca, *Catal. Today* 27 (1996) 497.
- [38] S.G. Masters, D. Chadwick, *Appl. Catal. B* 23 (1999) 235.
- [39] B. Shi, B.H. Davis, *J. Catal.* 157 (1995) 359.
- [40] A.R. McInroy, D.T. Lundie, J.M. Winfield, C.C. Dudman, P. Jones, S.F. Parker, J.W. Taylor, D. Lennon, *Phys. Chem. Chem. Phys.* 7 (2005) 3093.
- [41] F. Prinetto, G. Ghiotti, I. Nova, L. Lietti, E. Tronconi, P. Forzatti, *J. Phys. Chem. B* 105 (2001) 12732.
- [42] J.B. Peri, *J. Phys. Chem.* 69 (1965) 220.
- [43] H. Knozinger, P. Ratnasamy, *Catal. Rev. Sci. Eng.* 17 (1978) 31.
- [44] A.A. Tsyganenko, V.N. Filimonov, *J. Mol. Struct.* 19 (1973) 579.
- [45] W.F. Schneider, *J. Phys. Chem. B* 108 (2004) 273.
- [46] A.A. Davydov, *Molecular Spectroscopy of Oxide Catalyst Surfaces*, Wiley, New York, 2003, references therein.
- [47] J. Szanyi, J.H. Kwak, R.J. Chimentao, C.H.F. Peden, *J. Phys. Chem. C* 111 (2007) 2661.
- [48] N.W. Cant, D.C. Chambers, I.O.Y. Liu, *Appl. Catal. B* 46 (2003) 551.
- [49] M.L. Unland, *Science* 179 (1973) 567.
- [50] E. Ozensoy, D.W. Goodman, *Phys. Chem. Chem. Phys.* 6 (2004) 3765, references therein.
- [51] F. Solymosi, T. Bansagi, *J. Catal.* 202 (2001) 205, references therein.